

Modeling of time-lapse seismic reflection data from CO₂ sequestration at West Pearl Queen Field

Lewis C. Bartel, Matthew M. Haney, David F. Aldridge, Neill P. Symons, and Gregory J. Elbring
Geophysics Department, Sandia National Laboratories, Albuquerque, New Mexico



Introduction

Sequestration of CO₂ in depleted oil reservoirs, saline aquifers, or unminable coal sequences may prove to be an economical and environmentally safe means for long-term removal of carbon from the atmosphere. Requirements for storage of CO₂ in subsurface geologic repositories (e.g., less than 0.1% per year leakage) pose significant challenges for geophysical remote sensing techniques. The many issues relevant to successful CO₂ sequestration (volume in place, migration, leakage rate) require improved understanding of the advantages and pitfalls of potential monitoring methods. Advanced numerical modeling of time-lapse seismic reflection responses offers a controlled environment for testing hypotheses and exploring alternatives. The U.S. Department of Energy has conducted CO₂ sequestration and monitoring tests at West Pearl Queen (WPCQ) field in southeastern New Mexico (see below, Figure A). High-quality 3D seismic reflection data were acquired before and after injection of ~2 kt of CO₂ into a depleted sandstone unit at ~4200 ft depth. Images developed from time-lapse seismic data appear to reveal strong reflectivity changes attributed to displacement of brine by CO₂ (see below, Figure B). We are pursuing seismic numerical modeling studies with the goal of understanding and assessing the reliability and robustness of the time-lapse reflection responses.

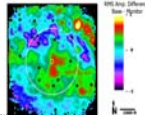


Figure A. Location of sequestration project near Hobbs, New Mexico.

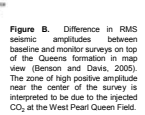


Figure B. Difference in RMS seismic amplitudes between baseline and monitor surveys at top of the Queen formation in main view (Eaton and Davis, 2005). The zone of high positive amplitude near the center of the survey is interpreted to be due to the injected CO₂ at the West Pearl Queen Field.

Seismic model construction

Well log information is used to construct a preliminary one-dimensional (1D) layered model for the WPCQ site, prior to introduction of CO₂ (Figure 1). The CO₂ sequestration reservoir is the Shattuck sandstone member of the Queen formation (a Central Basin Platform dolomite with numerous interbedded sands), occupying the depth interval ~1365 m to ~1383 m below surface. After CO₂ injection, seismic wave speeds are reduced by ~5–6%, as suggested by laboratory measurements tabulated in Wang et al. (1998). Mass density of the CO₂-saturated sandstone is estimated by assuming complete replacement of brine pore fluid by CO₂ within a medium of porosity $\phi = 0.16$ (Figure 2). The vertical variation in compressional (P) wave speed V_p , shear (S) wave speed V_s , and mass density ρ are subsequently extended to 3D spatial grids for use in the FD wave propagation algorithm. Figure 3 illustrates a 3D post-CO₂-injection P-wave speed model, where a uniform reduction in V_p is distributed within a 300 m × 600 m rectangular zone centered on the injector well.

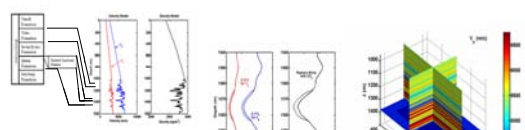


Figure 1. Vertical profiles of compressional wave speed (V_p), shear wave speed (V_s), and mass density (ρ) developed for the WPCQ site CO₂ sequestration site. Well log information from the Shattuck well is used to construct these profiles over the depth interval ~1025 m to ~1650 m. Compressional wave speed is then linearly extrapolated to the surface such that the normal incidence P-P reflection traveltimes from the Queen formation P ~0.640 seconds. Shear wave speed profiles in the overburden is obtained by linearly extrapolating the logge value at top of Yates formation to the surface value $V_s = 0.6071 V_p$. Finally, overburden mass density is generated via a Gardner-style relation. Depths of top of Yates, Shattuck, Queen, and Grayburg formations in the Central Basin Platform stratigraphic column are indicated. The Shattuck Sandstone member of the kick (downward lower) velocity of V_p , V_s , and ρ .

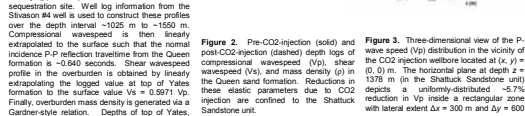
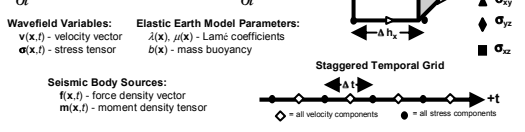


Figure 2. Three-dimensional view of the P-wave speed (V_p) distribution in the vicinity of the CO₂ injection wellbore located at $(x, y) = (0, 0)$ m. The horizontal plane at depth $z = 1378$ m (in the Shattuck Sandstone unit) depicts a uniformly distributed ~5.7% reduction in V_p inside a rectangular zone with lateral extent $\Delta x = 300$ m and $\Delta y = 600$ m.

Velocity-Stress Elastodynamic System and Finite-Difference Grid

Nine, coupled, first-order, non-homogeneous, partial differential equations:

$$\frac{\partial \mathbf{v}}{\partial t} - \mathbf{b}(\nabla \cdot \boldsymbol{\sigma}) = \mathbf{b}(\mathbf{f} + \mathbf{V} \cdot \mathbf{m})$$

$$\boldsymbol{\sigma} - \lambda(\nabla \cdot \mathbf{v}) \mathbf{I} - \mu(\nabla \mathbf{v} + \nabla \mathbf{v}^T) = \frac{\partial \mathbf{m}}{\partial t}$$


Wavefield Variables: $\mathbf{v}(x, t)$ - velocity vector
 $\boldsymbol{\sigma}(x, t)$ - stress tensor
Elastic Earth Model Parameters: $\lambda(x, t)$, $\mu(x, t)$ - Lamé coefficients
 $\mathbf{b}(x)$ - mass buoyancy
Seismic Body Sources: $\mathbf{f}(x, t)$ - force density vector
 $\mathbf{m}(x, t)$ - moment density tensor

3D velocity-stress system is numerically solved with an explicit, time-domain, O(2,4) staggered-grid, FD algorithm

Seismic data modeling

Synthetic seismic data are calculated with a time-domain, finite-difference (FD) numerical algorithm, appropriate for 3D wave propagation within a heterogeneous and isotropic elastic medium. All of the common seismological phases (P-waves, S-waves, reflections, refractions, mode-conversions, primaries, multiples, surface waves, diffractions, scattered arrivals, etc) are simulated with fidelity, provided spatial and temporal grid intervals are sufficiently fine. The large scale of these simulations mandates use of a massively-parallel computational implementation of the algorithm. The 3D numerical grid used for FD modeling consists of $351 \times 501 \times 803 = 141.2$ million gridpoints with spatial intervals $\Delta x = \Delta y = \Delta z = 2$ m. Seismic trace duration is 1.5 s, equivalent to 15,001 FD timesteps with a temporal interval $\Delta t = 0.1$ ms.

Figure 4 depicts a small portion of the field data acquisition geometry of the WPCQ field time-lapse seismic surveys. A complete computational replication of the seismic data generated by all of these sources is beyond the scope of the current investigation. Rather, we calculate five gathers of seismic traces generated by the particular sources indicated by large red dots in Figure 4. Each source is modeled as a buried vertical force (1 m deep), and the source waveform is a Ricker wavelet with peak frequency 25 Hz (1% amplitude bandwidth ~1.70 Hz). Receivers are three-component (3C) particle velocity sensors, also placed 1 m below the horizontal stress-free surface of the earth.

Synthetic seismic data are generated for both the pre-CO₂-injection and post-CO₂-injection earth models. At normal plot scales, only subtle differences in the calculated traces are discernible. However, after subtracting the traces, the expression of the CO₂-altered zone at depth is quite evident. Figure 5 displays the difference (post-injection minus pre-injection) of the vertical component (Vz) seismograms recorded by a central north-south (y-direction) line of 81 receivers; the seismic energy source is positioned at $(x, y) = (0, -400)$ m (lower large red dot in Figure 4). The strong event with zero-offset arrival time ~0.640 s is due to CO₂-alteration. All seismic reflections from interfaces above this zone (as well as horizontally-propagating surface waves, and many FD grid boundary reflections) disappear in the subtraction process.

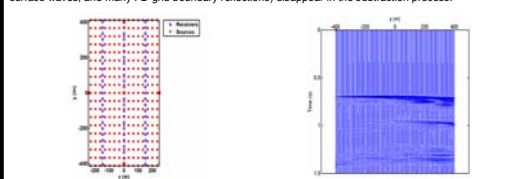


Figure 4. Surface deployment of seismic energy sources (red dots) and receivers (blue dots) in the vicinity of the CO₂ injector wellhead for the WPCQ field time-lapse seismic reflection surveys. The large red dot indicates energy source used to calculate synthetic seismic reflection data. Subsequent source locations are indicated.

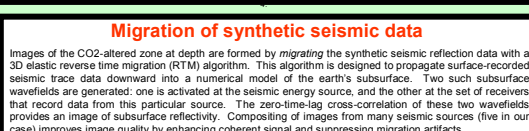


Figure 5. Synthetic seismic reflection data calculated with a 3D time-domain finite-difference (FD) elastic wave propagation algorithm. Traces depict the difference (post-CO₂ injection minus pre-CO₂ injection) in vertical particle velocity (V_z) recorded at surface receivers. The seismic energy source (red dot) is positioned at $(x, y) = (0, -400)$ m, and the line of 81 receivers extends from $\Delta x = -400$ m to $\Delta x = 400$ m in Figure 4.

Migration of synthetic seismic data

Images of the CO₂-altered zone at depth are formed by migrating the synthetic seismic reflection data with a 3D elastic reverse time migration (RTM) algorithm. This algorithm is designed to propagate surface-recorded seismic trace data downward into a numerical model of the earth's subsurface. Two such subsurface wavefields are generated; one is activated at the seismic energy source, and the other at the set of receivers that record data from this particular source. The zero-time-lag cross-correlation of these two wavefields provides an image of subsurface reflectivity. Compositing of images from many seismic sources (five in our case) improves image quality by enhancing coherent signal and suppressing migration artifacts.

We apply reverse time migration to the synthetic seismic data generated from both the pre-injection and post-injection models of the WPCQ CO₂ sequestration site. Figure 6 illustrates time-lapse images on selected horizontal planes within the Shattuck sandstone unit of the Queen formation. Each image is obtained by subtracting the pre-CO₂-injection migrated image from the corresponding post-CO₂-injection image. There is a clear response due to CO₂-alteration of elastic parameters. Although this response is (correctly) centered on the injector well, edge definition is diffuse and ambiguous (compare time-lapse images with the uniformly distributed rectangular Vp-reduction zone in the lower right panel of Figure 6).

A similar synthetic modeling and migration experiment has been performed with a spatially-variable CO₂-altered zone within the Shattuck sandstone. A 3D fractal distribution of elastic parameters (Figures 7 and 8) mimics a geologically-realistic sinuous channel sand environment within the Queen formation. These channels may form preferred flow pathways for the injected CO₂. A comparison of time-lapse migrated images on the same depth plane for the fractal and uniform reductions in elastic parameters is illustrated in Figure 9. Clearly, the fractal distribution reduces the overall amplitude of the image response, as well as introducing an asymmetry related to the underlying geometry of the medium parameters. The 3D image comparison illustrated in Figure 10 also indicates lower-amplitude response associated with the fractal model.

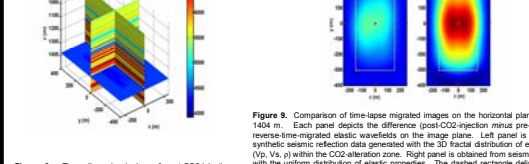


Figure 6. Comparison of time-lapse migrated images on the horizontal plane with depth $z = 1404$ m. Each panel depicts the difference (post-CO₂ injection minus pre-CO₂ injection) in the obtained time-lapse images. Left panel is constructed from synthetic seismic reflection data generated with the 3D fractal distribution of elastic parameters (V_p, V_s, ρ) within the CO₂-alteration zone. Right panel is obtained from seismic data calculated with the uniform distribution of elastic properties. The dashed rectangle delineates the lateral extent of the CO₂-alteration zone within the Shattuck Sandstone. Seismic reflection data are calculated for five energy sources located on the surface at the red dots. As expected, the amplitude of the time-lapse image generated from the fractal model is reduced, compared with the uniform model. Additionally, a slight asymmetry is discernible in the image from the fractal model.

Static shift experiments

Highly repeatable field data acquisition parameters and conditions are essential for effective time-lapse seismic reflection surveying. In order to correctly interpret the processed seismic data, all observed changes in the data should be attributed to changes in subsurface earth properties that take place between surveys. However, as a practical matter, it is difficult to exactly replicate the original source and receiver locations and earth coupling conditions on the second seismic survey. Additionally, changes in the shallow subsurface weathered zone, generated say by increased/decreased moisture content, may obscure a proper interpretation of the time-lapse data. We examine these effects by introducing static time shifts into the post-injection seismic data generated from the uniformly-distributed (Vp, Vs, ρ) CO₂-alteration model. These shifts are designed to simulate data differences arising from the aforementioned effects. The 2D spatial distribution of the time shifts mimics a realistic surface consistent static situation; all traces generated from the same source location are shifted by an identical amount, and all traces recorded at the same receiver location are shifted by an identical (but different) amount. Time shifts are drawn from a zero-mean, rectangular random distribution with specified maximum value.

Figure 11 displays time-lapse migrated images resulting from this study. Clearly, larger magnitude shifts lead to a progressive degradation in image quality, in both amplitude and shape. With time shifts as large as 5% (of the one-way traveltime through an assumed shallow subsurface weathered zone), the resulting time-lapse image on the horizontal plane with the Shattuck sandstone becomes uninterpretable. Finally, Figure 12 clearly indicates that time shifts lead to a significant degradation in image quality throughout the 3D image volume. Our conclusion is that variations between the two field surveys must be minimized during data acquisition, and that the time-lapse seismic data must be carefully processed to eliminate any residual differences not attributable to the changed earth model.

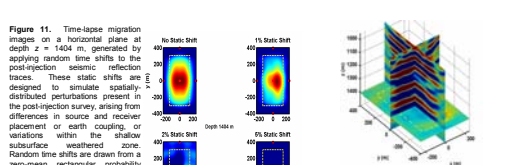


Figure 11. Time-lapse migration images on a horizontal plane at depth $z = 1404$ m, generated by applying random time shifts to the synthetic seismic reflection traces. These static shifts are designed to simulate spatially-distributed perturbations present in the post-injection survey, arising from the aforementioned effects. Random time shifts are drawn from a zero-mean rectangular probability distribution, with maximum value equal to a specified percentage of one-way traveltime through an assumed 200 m thick weathered zone. Clearly, larger magnitude shifts result in a progressive degradation of image quality. As indicated previously, the red dots denote locations of five seismic energy sources used to calculate the synthetic seismic reflection data, and the dashed rectangle outlines the extent of spatially-uniform alteration in elastic medium parameters (V_p, V_s, ρ). The static shifts create a significant degradation in image quality throughout the 3D volume. In particular, a large-amplitude oscillatory response (red/blue = positive/negative) is evident above the CO₂ injection zone.

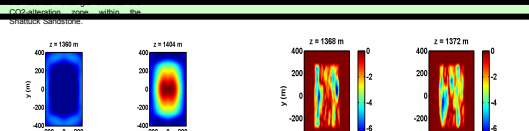


Figure 12. Three-dimensional view of the time-lapse migration volume generated from the post-injection seismic reflection dataset with 2% static time shifts applied. The horizontal plane at depth $z = 1404$ m is located within the Shattuck Sandstone CO₂-injection zone; dashed rectangle outlines the extent of spatially-uniform alteration in elastic medium parameters (V_p, V_s, ρ). The static shifts create a significant degradation in image quality throughout the 3D volume. In particular, a large-amplitude oscillatory response (red/blue = positive/negative) is evident above the CO₂ injection zone.

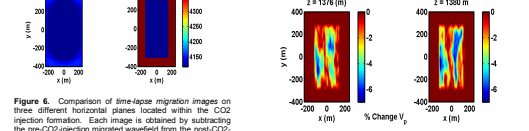


Figure 7. Comparison of time-lapse migration images on three different horizontal planes located within the CO₂ injection formation. Each image is obtained by subtracting the pre-CO₂-injection migrated wavefield from the post-CO₂-injection migrated wavefield. The three images are plotted with the same color amplitude scale (red/blue = positive/negative). Lower right panel illustrates a uniform reduction in P-wave speed on the horizontal plane at depth $z = 1378$ m. Ideally, the time-lapse images should conform with this rectangle. Differences arise from the small number of seismic energy sources and receivers utilized in the reverse-time migrations, their restricted spatial aperture, and the limited spectral bandwidth of the propagating seismic waves.

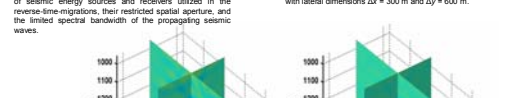


Figure 8. Comparison of three-dimensional time-lapse migration images for the uniform CO₂ alteration model (left) and the fractal CO₂ alteration model (right). Both images are plotted with the same color amplitude scale, with green indicating null (i.e., zero difference). Clearly, the uniform distribution model generates a larger amplitude response on the horizontal plane at depth $z = 1404$ m.

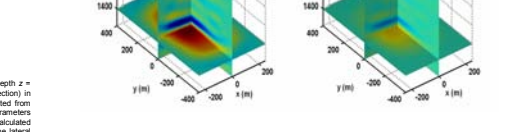


Figure 9. Percent change in P-wave speed (V_p) for a fractal distribution model on four horizontal planes within the Shattuck Sandstone unit of the Queen formation. Spatially-variable reductions in V_p are confined to the injection zone with lateral dimensions $\Delta x = 300$ m and $\Delta y = 600$ m.

Layered medium modeling

Since the stratigraphy at WPCQ field (and indeed most of the Permian Basin of West Texas and Southeast New Mexico) is well-approximated by a sequence of horizontal layers, we are currently developing a fast forward modeling code that exploits advantages in modeling for 1D layered media. This capability enables rapid calculation of, for instance, amplitude vs. offset (AVO) seismic reflection responses in a single-processor workstation computational environment. AVO analysis of seismic reflections is widely practiced in the petroleum industry, and is used to infer lithologic and/or fluid saturation parameters of a petroleum reservoir. Although the specialization to a 1D layered earth model is a restriction, it allows exploitation of efficient numerical procedures enabling extremely rapid calculations. Seismic wavefield simulations can be conducted in a matter of minutes, rather than hours.

A sample source gather of pressure traces, calculated for an identical earth model and recording geometry used for a run with the 3D FD algorithm, is displayed in Figure 14. Apart from a very small amplitude imbalance, the traces illustrated in Figures 13 and 14 are virtually identical. This provides assurance that our two computational algorithms are valid. The current algorithm implementation utilizes acoustic (i.e., ideal fluid) layers. Future plans are to upgrade the approach to accommodate solid elastic layers, so that shear and mode-converted seismic phases can be accurately modeled.

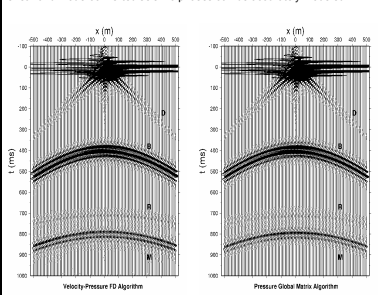


Figure 13. Source gather of pressure traces calculated with 3D velocity-pressure finite-difference acoustic wave propagation algorithm. Earth model and data recording configuration is exactly the same as for a run with the 3D FD algorithm. Traces are virtually identical to those displayed in Figure 13 (and calculated by an entirely different numerical algorithm).

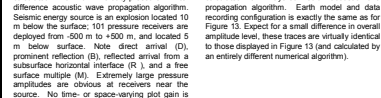


Figure 14. Source gather of pressure traces calculated with 3D velocity-pressure finite-difference acoustic wave propagation algorithm. Earth model and data recording configuration is exactly the same as for a run with the 3D FD algorithm. Traces are virtually identical to those displayed in Figure 13 (and calculated by an entirely different numerical algorithm).

Discussion, Conclusions, Future Directions

Utilizing a 3D time-domain finite-difference synthetic elastic wave propagation algorithm, we are capable of generating realistic synthetic data at WPCQ field. With this capability, we examine how various types of errors and noise in the 4D data degrade the ability to image a deep CO₂ plume. Source/receiver sampling, subsurface illumination, correlated geologic heterogeneity, and static shifts are considered. As a result, we are able to make quantitative estimates of the tolerable errors for monitoring CO₂ injection at WPCQ field. Due to the strong sensitivity of the time-lapse images on static errors, some receivers used for CO₂ monitoring may need to be located below the complex and variable near-surface layer. We plan in the future to consider fully 3C time-lapse data (which exists at WPCQ) in the numerics, modeling, as well as statistical models of the Shattuck Sandstone to more realistically represent reservoir complexity.

Ultimately, we intend to simulate seismic reflection data at the WPCQ field CO₂ sequestration site with a poroelastic wave propagation algorithm, based on Biot's dynamic equations governing wave propagation within a fluid-saturated porous solid. This algorithm, also developed in the SNL Geophysics Department, allows quantitative prediction of effects on seismic data due to various subsurface fluid and flow parameters such as porosity, fluid type, saturation, permeability, pore structure tortuosity, fluid viscosity, etc, without resorting to effective medium elastic assumptions. Since numerical solution of Biot's poroelastic equations is considerably more demanding than in elastodynamics, our massively-parallel version of the velocity-stress-pressure finite-difference algorithm (Aldridge et al., 2005) must be employed.

REFERENCES
Aldridge, D.F., Symons, N.P. and Bartel, L.C., 2005. Poroelastic wave propagation with a velocity-stress-pressure algorithm. *Proceedings of the Third International Conference on Poroelasticity*, University of Oklahoma, Norman, OK, 24-27 May 2005, pages 293-295.
Eaton, R.D. and Davis, T.L., 2005. CO₂ Sequestration in a Depleted Oil Reservoir - West Pearl Queen Field. 67th EAGE Conference and Exhibition, June 13-16, Madrid, Spain, P37.
Malinver, C., 2004. Statistical Applications to Quantitative Seismic Reservoir Characterization and Monitoring at West Pearl Queen Field. *Lea County, New Mexico*. MSc. Thesis, Colorado School of Mines.
Wang, Z., Cates, M.E., and Langan, R.T., 1998. Seismic monitoring of a CO₂ flood in a carbonate reservoir: a rock physics study. *Geophysics*, 63, 1604-1617.